

Journal of Biomedical Optics

SPIEDigitalLibrary.org/jbo

Low-level laser therapy on MCF-7 cells: a micro-Fourier transform infrared spectroscopy study

Taciana D. Magrini
Nathalia Villa dos Santos
Marcella Pecora Milazzotto
Giselle Cerchiaro
Herculano da Silva Martinho

Low-level laser therapy on MCF-7 cells: a micro-Fourier transform infrared spectroscopy study

Taciana D. Magrini, Nathalia Villa dos Santos, Marcella Pecora Milazzotto, Giselle Cerchiaro, and Herculano da Silva Martinho

Universidade Federal do ABC, Centro de Ciências Naturais e Humanas, Rua Santa Adélia 166, Bangu, Santo André, SP, 09210-170, Brazil

Abstract. Low-level laser therapy (LLLT) is an emerging therapeutic approach for several clinical conditions. The clinical effects induced by LLLT presumably scale from photobiostimulation/photobioinhibition at the cellular level to the molecular level. The detailed mechanism underlying this effect remains unknown. This study quantifies some relevant aspects of LLLT related to molecular and cellular variations. Malignant breast cells (MCF-7) were exposed to spatially filtered light from a He-Ne laser (633 nm) with fluences of 5, 28.8, and 1000 mJ/cm². The cell viability was evaluated by optical microscopy using the Trypan Blue viability test. The micro-Fourier transform infrared technique was employed to obtain the vibrational spectra of each experimental group (control and irradiated) and identify the relevant biochemical alterations that occurred due to the process. It was observed that the red light influenced the RNA, phosphate, and serine/threonine/tyrosine bands. We found that light can influence cell metabolism depending on the laser fluence. For 5 mJ/cm², MCF-7 cells suffer bioinhibition with decreased metabolic rates. In contrast, for the 1 J/cm² laser fluence, cells present biostimulation accompanied by a metabolic rate elevation. Surprisingly, at the intermediate fluence, 28.8 mJ/cm², the metabolic rate is increased despite the absence of proliferative results. The data were interpreted within the retrograde signaling pathway mechanism activated with light irradiation. © 2012 Society of Photo-Optical Instrumentation Engineers (SPIE). [DOI: 10.1117/1.JBO.17.10.101516]

Keywords: low-level laser therapy; Fourier transform infrared; cancer; phototherapy; retrograde signaling pathway.

Paper 11734SSP received Dec. 9, 2011; revised manuscript received Jun. 14, 2012; accepted for publication Jun. 18, 2012; published online Aug. 3, 2012.

1 Introduction

Low-level laser therapy (LLLT) is a type of therapy that uses low-dose laser irradiation of less than 1 J/cm² in tissues, mainly to repair the tissues.¹ The reported effects include reduction of the postinjury inflammatory process, acceleration of soft tissue healing, and stimulation of the formation of new blood vessels.² The interaction between light and cells can result in molecular-, cellular-, and tissue-level effects, but the response of the cell to laser biostimulation is variable and diverse.^{2,3} It is well established that photons in the red or near-infrared (IR) induce the strongest effects and are predominantly absorbed in the mitochondria. Once absorbed, the IR photons activate several signaling ways, most of which have not yet been experimentally observed. The work of Karu⁴ summarized several experimental findings and proposed a mechanism of light-cell interaction that is one of the most cited mechanisms in the literature. It is based on retrograde signaling activated with light irradiation in the visible and infrared.⁴⁻⁶ The putative schematic signaling mechanism is shown in Fig. 1 (as adapted from Ref. 5). The process begins with the absorption of a photon with energy $h\nu$ by the photoacceptor cytochrome c oxidase.^{7,8} It is well documented in models of isolated mitochondria and whole cells that monochromatic light excitation affects the mitochondrial membrane potential ($\Delta\psi_m$), which drives the synthesis of ATP.⁹ Other characteristic changes are observed in the concentration of reactive oxygen species (ROS),¹⁰⁻¹² Ca²⁺,¹³ and NO.^{4,12} Mitochondria also have the capacity to communicate with the nucleus by structural changes

in the organelle itself. One way to communicate is by changes in the fission-fusion homeostasis (ΔFFH) in a dynamic mitochondrial network.¹⁰ Mitochondrial ultrastructure suffers alterations upon exposure to light stimuli.¹⁴ As a result, changes are induced in the ATP synthesis,¹⁰ the intracellular redox potential (E_h),^{4,15} pH,¹⁰ and cyclic adenosine monophosphate (cAMP).¹⁶ Several experiments have demonstrated that the membrane permeability and ion flux at the cell membrane (ΔE_m) are altered while changes in the nuclear factor kappa B (NF κ B) and activate protein-1 (AP-1) occur as a response to these factors.^{4,17} These experimentally shown pathways are indicated by continuous arrows in Fig. 1. Karu suggested some complementary or alternative pathways, which are indicated by dashed arrows and include the direct upregulation of various genes following mitochondrial stimuli or via NF κ B, AP-1, or ΔE_m .

The metabolic responses of cells can be probed by analytical techniques such as vibrational spectroscopy.^{17,18} Fourier transform infrared (FTIR) spectroscopy can provide some information to identify cells that are in specific phases of the cell cycle¹⁹ and to provide qualitative information on various vibrational transitions that give a detailed fingerprint of different bonds, functional groups, and conformations of molecules and biopolymers. Furthermore, FTIR spectroscopy is a quantitative tool that can obtain an estimation of the quantities of molecules and eventually establish a metabolic fingerprint of the cells.²⁰ Activation or inhibition of metabolism by irradiation (632.8 nm) has been observed by Karu for a yeast culture where protein synthesis depends on the light dose.²¹

It is clear that more experimental work must be performed to verify the correctness of the proposed pathways and to

Address all correspondence to: Herculano da Silva Martinho, Universidade Federal do ABC, Centro de Ciências Naturais e Humanas, Rua Santa Adélia 166, Bangu, Santo André, SP, Brazil 09210-170. Tel: 55-11-49960173; E-mail: herculano.martinho@ufabc.edu.br

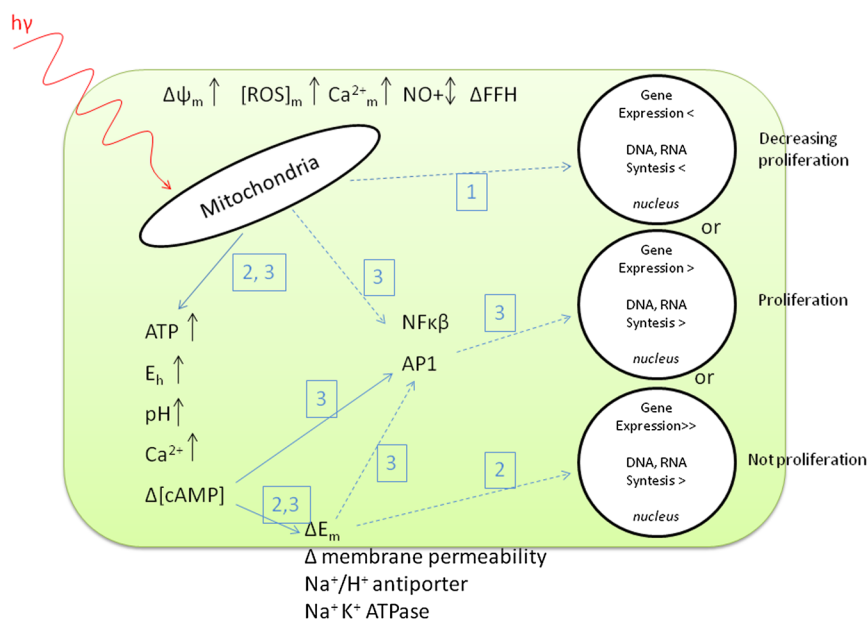


Fig. 1 Scheme of mitochondrial retrograde signaling pathways as proposed by Ref. 4. This illustration was adapted from Fig. 1 of Ref. 4 and shows three different mechanisms of action based on our results. See text for details.

consolidate the others. The fluences that lead to the best biostimulation or bioinhibition are not well established in the literature²² because it depends on many variables such as the cell type, wavelength, intensity, power laser, irradiation time, and others. For this determination, the greatest reproducibility possible for the experimental setup for the photo-stimulation experiment is necessary.

The present study is a survey of the biochemical and proliferative alterations induced by LLLT on tumor epithelial cells MCF-7. This cell line is a standard model that can be used for the study of breast cancer. However, it is known that cancer cells exhibit atypical behavior because the cancer promoter genes, the oncogenes, are generally activated in the cancer cells, giving them new properties, such as over-proliferation and accelerated growth compared with normal cells.²³ In the case of the MCF-7 cells, the tendency for over-proliferation is manifested by the WNT7B oncogene.²⁴ Thus it is important draw attention to the fact that the response of this cell line to the light maybe different than that of normal cells, and comparison between them might not be possible.

The main objective of the present work is to contribute to the understanding of the light-tissue interaction in the case of malignant cells (MCF-7 cells) and to compare the results with the work of Karu et al.⁴ This work could help to illuminate the obscure mechanisms underlying these interactions, which could be important for understanding the synergy between photobiostimulation/inhibition and photosensitizer action. The other important goal of this study is to determine a standardized experimental setup for this type of study to give us precise information about the exact quantity of light delivered to the cells.

2 Materials and Methods

2.1 Cell Culture

MCF-7 mammary adenocarcinoma cell (American Type Culture Collection, ATCC) monolayer cultures were grown in RPMI-1640 culture medium (SigmaAldrich), complemented with

10% of fetal bovine serum (v/v) (Gibco), 5 mg/ml of insulin (SigmaAldrich), 100 U/ml of penicillin, and 100- μ g/ml streptomycin (SigmaAldrich). Cell media were prepared with DNase- and RNase-free water and filtered through 0.22- μ m filter membranes (Millex@GV, Millipore) prior to use. Cell cultures were manipulated using sterile, disposable, nonpyrogenic plasticware and were maintained at 37 °C in an atmosphere of 5% CO₂ in air at a relative humidity of 80%. The cells were examined using an inverted microscope (400x Olympus IX71) and were subcultured according to protocols described by the ATCC.²⁴

2.2 Trypan Blue Exclusion Test

The Trypan Blue exclusion test was performed to assess the effects of the light on cell viability every 24 h after irradiation. Typically, cells were plated onto the medium at a density of 1.71×10^4 cells/cm² to give monolayers of approximately 30% cell confluence and incubated for 48 h under the conditions stated above. Following 24 h of incubation, cells were irradiated and trypsinized (1:4 PBS EDTA), and the adherent cells were combined and washed with phosphate buffered saline (PBS: 137 mM NaCl and 2.7 mM KCl in 10 mM phosphate buffer at pH 7.4); a 20- μ l sample (with a PBS dilution) of cells stained with Trypan blue (10:8 PBS) was counted under an optical microscope using a Neubauer chamber.

2.3 Irradiation

Irradiation was performed with a He-Ne laser (TEM00, Unilaser, Brazil) at a wavelength of 633 nm and an output power of 24 mW. Three experiments were performed in quadruplicate with fluences of 5, 28.8, and 1000 mJ/cm² \pm 30% with a single dose of light applied 24 h after the cells were plated. The irradiation parameters are shown in Table 1. The typical wavefront at the laser exit had a Gaussian shape. To homogenize the wavefront intensity distribution within the circular area (9.8 cm²) of the six-well culture plate, the light was passed through a

Table 1 Irradiation parameters.

Fluence (mJ/cm ²)	5	28.8	1000
Power (mW)	1.3	7.5	15
Power density (mW/cm ²)	0.083	0.48	0.97
Irradiation time (min)	1	1	16.5
Number of experiments	4	4	4
Time of evaluation for counting (h)	24	24	24
Time of evaluation for spectroscopy (h)	12	12	12
Area of irradiation per well (cm ²)	9.8	9.8	9.8

homemade spatial filter designed for this purpose. The filter was composed of two plan-concave, 150-mm focal distance lenses, a pinhole with a diameter of 0.23 mm, a bi-concave lens and optical filters that were used to regulate the power of the laser according to the dose. The beam light power was verified with a power-meter (Newport 841-PE). A 45-deg mirror deflected the light beam to the individual cell wall plate [see Fig. 2(a)]. The light intensity distribution was checked through a CCD camera (Samsung NV8, 8 MP digital camera) placed perpendicular to the beam. The exit signal of the CCD was analyzed by ImageJ software. The net delivered power within the well was calculated from the radial intensity distribution [Fig. 2(b)]. The MCF-7 cells were seeded at a final concentration of approximately 1.71×10^4 cells/cm² (30% confluence in six-well plate), incubated for 24 h to allow the cells to attach and

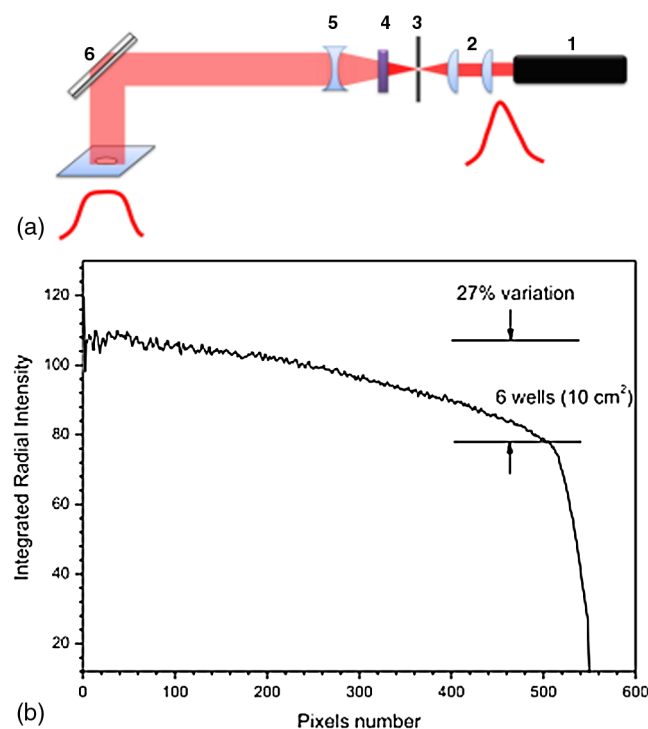


Fig. 2 (a) LLLT system setup. 1: He-Ne laser (633 nm). 2: Plan-concave lenses. 3: Pinhole. 4: Interferential filter. 5: Bi-convex lens. 6: Mirror. 7: Blackout. 8: Cell culture plate; and (b) Radial intensity distribution.

after irradiation. Thus the $t = 24$ h cells were plated, the $t = 0$ h cells were irradiated, and at $t = 12$ h, FTIR measurements were performed. The plate was covered with a blackout protection with a single hole to enable the illumination of a single well at a time. After irradiation, the medium was changed at $t = 120$ h.

2.4 Micro FTIR Spectroscopy

Spectra were collected every 12 h after irradiation. A Varian 610 FTIR Micro-spectrometer was used in reflectance mode, with a spectral resolution of 4 cm^{-1} , 200 scans per sample and 800 scans per background. The sample holder was a platinum recovered surface plate. An aliquot of $20 \mu\text{L}$ was deposited in the sample holder after it was trypsinized, centrifuged, and washed with PBS and the supernatant was removed. The cell pellet was conserved with a quantity of supernatant depending on the elapsed time (for 12 h, it was approximately $50 \mu\text{L}$ and, for 156 h, it was approximately $650 \mu\text{L}$) to ensure that all samples had similar cell concentrations. Samples contained PBS, but it does not cause noise; thus, after drying, the film samples were washed with deionized water, and then salt was removed. Three spectra per sample were obtained. Each one was baseline corrected manually with *Fityk* software and normalized to 1. Then the average spectrum was computed. The integrated area of the individual bands was plotted against time after normalization to the $t = 12$ h intensity for comparison.

2.5 Statistical Analysis

Student's t-test was used for the statistical analysis of cell counts and band intensities.

3 Results and Discussion

It was observed that the number of cells varied depending on the fluence (Fig. 3). Statistically, for the group exposed to 5 mJ/cm^2 , the greatest number of dead cells was observed at all times in the irradiated group except at 48 h. For the group exposed to 28.8 mJ/cm^2 , the number of dead cells was significantly greater in the irradiated group at 24 to 72 h. At other times (96 to 144 h), no significant effects in proliferation were observed. For the 1 J/cm^2 fluence, the number of dead cells was equal at all times except at 72 h, when the number was greater in the irradiated group. The group subjected to a fluence of 5 mJ/cm^2 generally presented significantly fewer cells than the control; the group subjected to a fluence of 28.8 mJ/cm^2 presented a quantity of cells equal to that of the control, and the group subjected to a fluence of 1 J/cm^2 presented a quantity of cells significantly greater than the control (Table 2 shows the results of the Student's t-test).

Figure 4 presents the box-plot of the spectra measured between 800 and 1800 cm^{-1} (finger print region). The spectral features observed are in agreement with those reported in the literature.^{20,25} Table 3 displays the main vibrational bands and the corresponding assignments. The intensity changes between the irradiated and control spectra (at all times) were analyzed by computing the integrated area of the main bands. The results of the Student's t-test applied to these bands are summarized in Table 3.

The time dependence of the integrated areas is shown in Figs. 5 to 7. The letters a, b, and c (horizontal series of graphs) indicate the results for 5 mJ/cm^2 , 28 mJ/cm^2 , and 1 J/cm^2

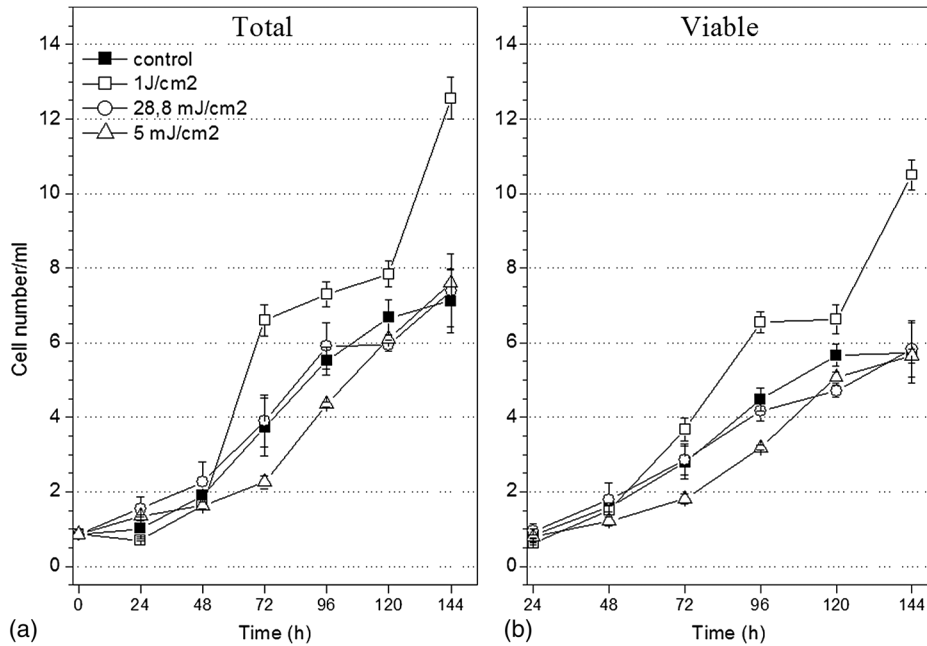


Fig. 3 Number of total and viable cells/ml with time for three fluences.

Table 2 Student's t-test results.

Time (h)	1 J/cm ²		28.8 mJ/cm ²		5 mJ/cm ²	
	<i>p</i> viable	<i>p</i> total	<i>p</i> viable	<i>p</i> total	<i>p</i> viable	<i>p</i> total
24	0.302	0.302	0.105	0.485	<0.05	<0.05
48	<0.05	<0.05	0.394	0.307	0.078	0.089
72	0.365	<0.05	0.359	0.228	<0.05	0.053
96	<0.05	<0.05	0.322	0.382	<0.05	0.050
120	0.286	0.097	<0.05	0.072	0.307	0.330
144	<0.05	<0.05	0.468	0.377	<0.05	<0.05

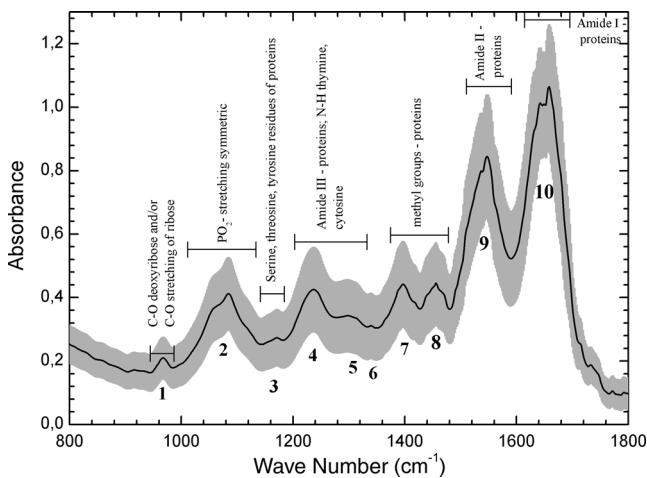


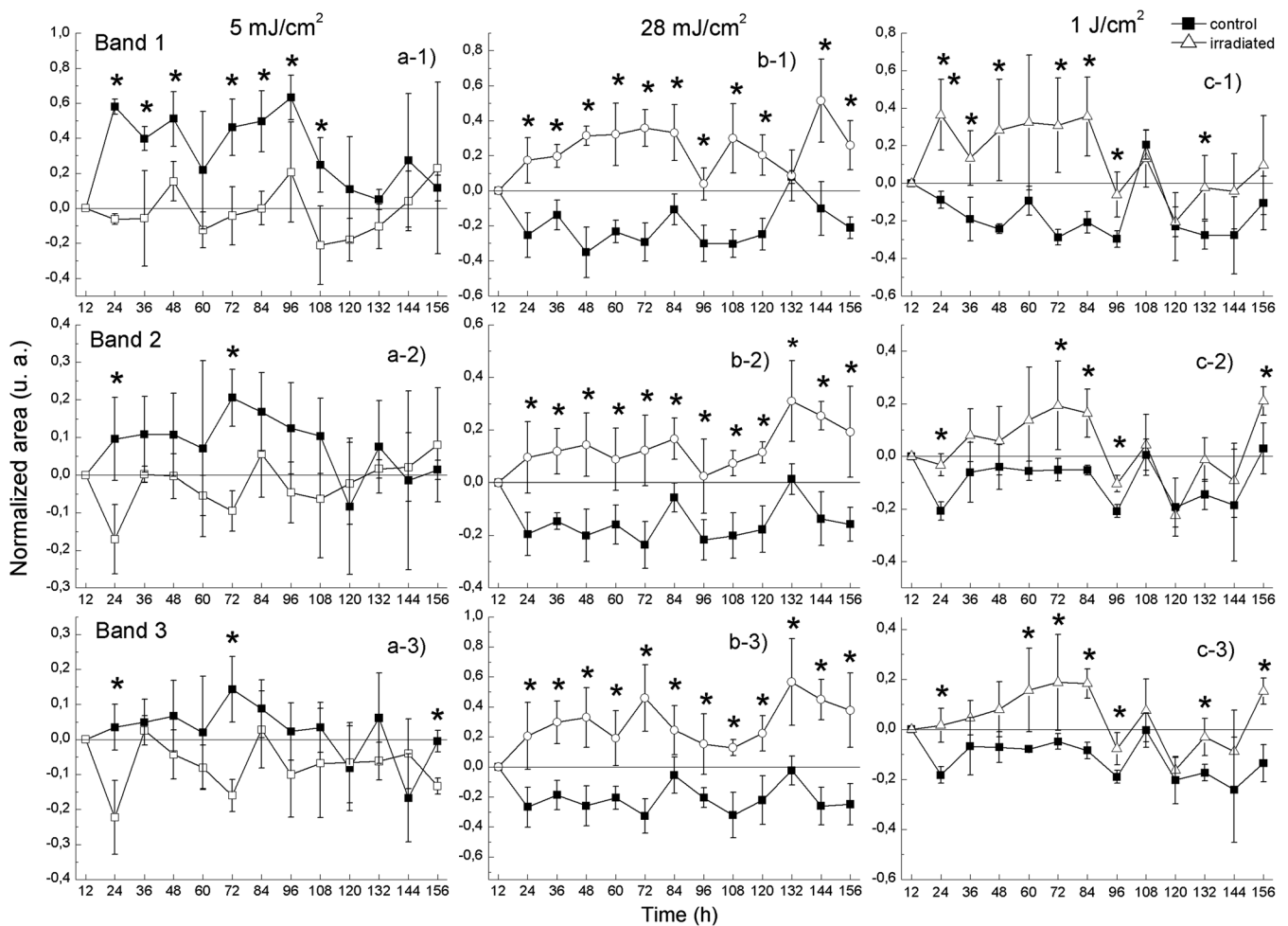
Fig. 4 FTIR box-plot spectra. The spectra were normalized to 1, and a nonlinear baseline was subtracted in the range of 800 to 4000 cm⁻¹. The corresponding assignment is shown in Table 3.

fluences, respectively. The vertical series present the data for different bands.

The almost periodic intensity variation in both control and irradiated groups could be due to the metabolic and structural changes occurring during the cell cycle phases.¹⁹ There is a normal distribution of cells in each phase of the cycle,²⁶ therefore it is our hypothesis that there was little variation in the distribution every 12 h, both in the control group and in the irradiated group. It is also known that plated cells all begin in the same cell cycle phase, and, after the initial cycle, their cycles can change depending on conditions such as environmental factors, which could explain the large variation between the quantities of the cell components between different fluences, even in the control group. However, the quantities of important components of the cell such as the DNA, RNA, and proteins of the irradiated cells undergo approximately the same changes (increases or decreases) in their intensities in relation to the control group over time but with some differences, especially in their quantity. Moreover, the irradiation had an influence on the cell component seven after six or seven days for each fluence.

Table 3 Assignment of vibrational bands following Ref. 22.

Bands	Spectral band (cm^{-1})	Molecules
1	966	C–O phosphodiester of deoxyribose and ribose, C–C of DNA 1057 cm^{-1} C–O stretching deoxyribose shoulder
2	1083	PO_2^- phosphodiester stretching symmetric of nucleic acids, DNA 1121 cm^{-1} phosphodiester shoulderRNA
3	1171	Stretching modes of C–OH groups of serine, threonine, tyrosine residues
4	1237	Amide III of proteins; asymmetric phosphodiester of phosphate of nucleic acids
5	1298	Unassigned band
6	1339	CH_2 wagging; collagen
7	1397	Symmetric bending methyl groups: proteins
8	1456	Asymmetric bending methyl groups: proteins
9	1546	Amide II ($\delta\text{N-H}$, $\nu\text{C-N}$) proteins
10	1657	($\nu\text{C}=\text{O}$, $\delta\text{C-N}$, $\nu\text{N-H}$) Amide I (α -helix) of proteins overlapping with the modes of nucleic acid

**Fig. 5** Normalized areas of bands 1, 2, and 3 with time, where the filled symbols are the control groups and the open symbols are the irradiated groups. Asterisks represent significant differences between the control and irradiated groups.

In this work, we present the results of a cell culture that increases in quantity (exponential and plateau phase at the seventh day for the control group, consistent with Ref. 27) and passes through the cell cycle (M, G1, S, and G2), but in the graphs of the band areas, we cannot see the increase of the areas over time due to the increase in quantity because the quantities of cells in the samples were standardized, and the spectra were post-processed. Nevertheless, we can estimate the variation in the quantity of proteins based in our results for the time dependence of bands 3, 4, 7, 8, 9, and 10 of DNA (bands 1, 2), RNA (band 2), serine, threonine, tyrosine (band 3), nucleic acids (bands 2, 4, 10) and collagen (band 6)²⁵ compared with the control group.

In the literature, it has been shown that it is possible to monitor metabolic processes in tissues and cells;¹⁷ additionally, in actively dividing or metabolically active cells, the spectral characteristics of RNA can show a high variation in the signal depending on the activity of the cell.²⁸ Furthermore, the content of proteins is expected to increase more or less continuously during the cell cycle,²³ therefore the estimation of proteins and nucleic acids shows a metabolic variation over time for the control group and the irradiated group for each fluence. Figures 6 and 7 show that the intensities of the irradiated groups are generally (i.e., in most bands) lower for the bands of the 5 mJ/cm² fluence samples and higher for the bands of the

samples treated with other fluences. The detailed analysis for each fluence will be discussed below.

3.1 Discussion for the Mechanism Occurring at a Fluence of 5 mJ/cm²

For a fluence of 5 mJ/cm² and a wavelength of 632.8 nm (6 mW output power, irradiation time of 15 s), the literature (Ref. 14) reports an increase of the intracellular concentration of [Ca²⁺]_i in the first minutes after irradiation in lymphocytes. In addition, there were verified changes in the structure of chromatin and an increase in the production of RNA in the first 7 h after irradiation, but there was no proliferation. This result reported in the literature shows us that, after irradiation, the cells had some modifications in metabolism, but these changes were not reflected in the proliferation of the cells. In contrast, in our results for this fluence and wavelength in MCF-7 cells, cell bioinhibition (i.e., a decrease of multiplication of cells with respect to the control group) occurred, and the areas of the bands were all less than those of the control group, especially bands related to the nucleic acids [DNA, band 1, Fig. 5(a-1)]. A greater amount of cell death occurred at all times compared with the control. There was only a slight decrease of the RNA [band 2, Fig. 5(a-2)] compared with the control for bands 3 and 4 [Fig. 5(a-3) and 6(a-4)]; these

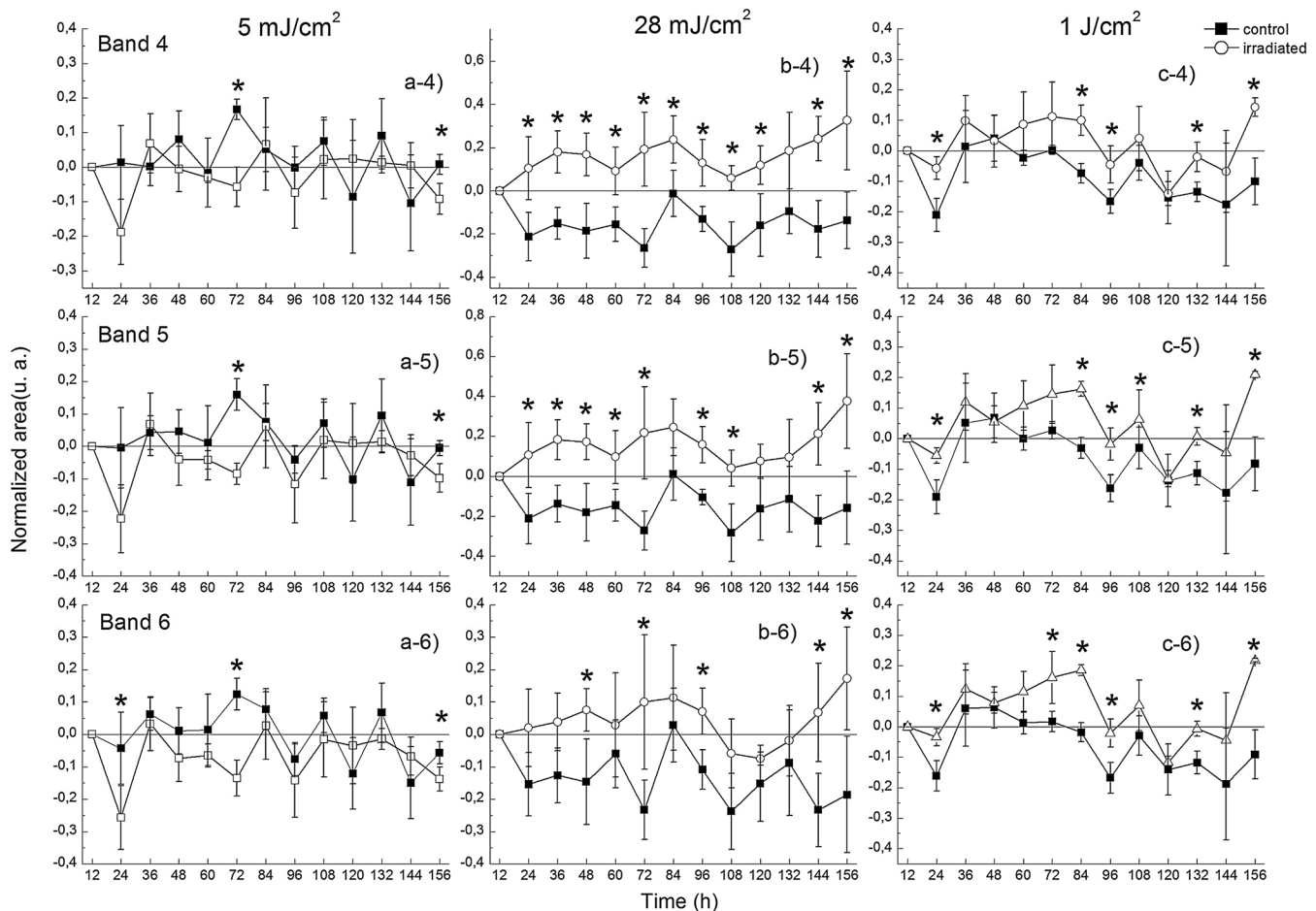


Fig. 6 Normalized areas of bands 4, 5, and 6 with time. The closed and open symbols represent the control and irradiated groups, respectively. Asterisks indicate the times when significant differences between the control and irradiated groups were detected.

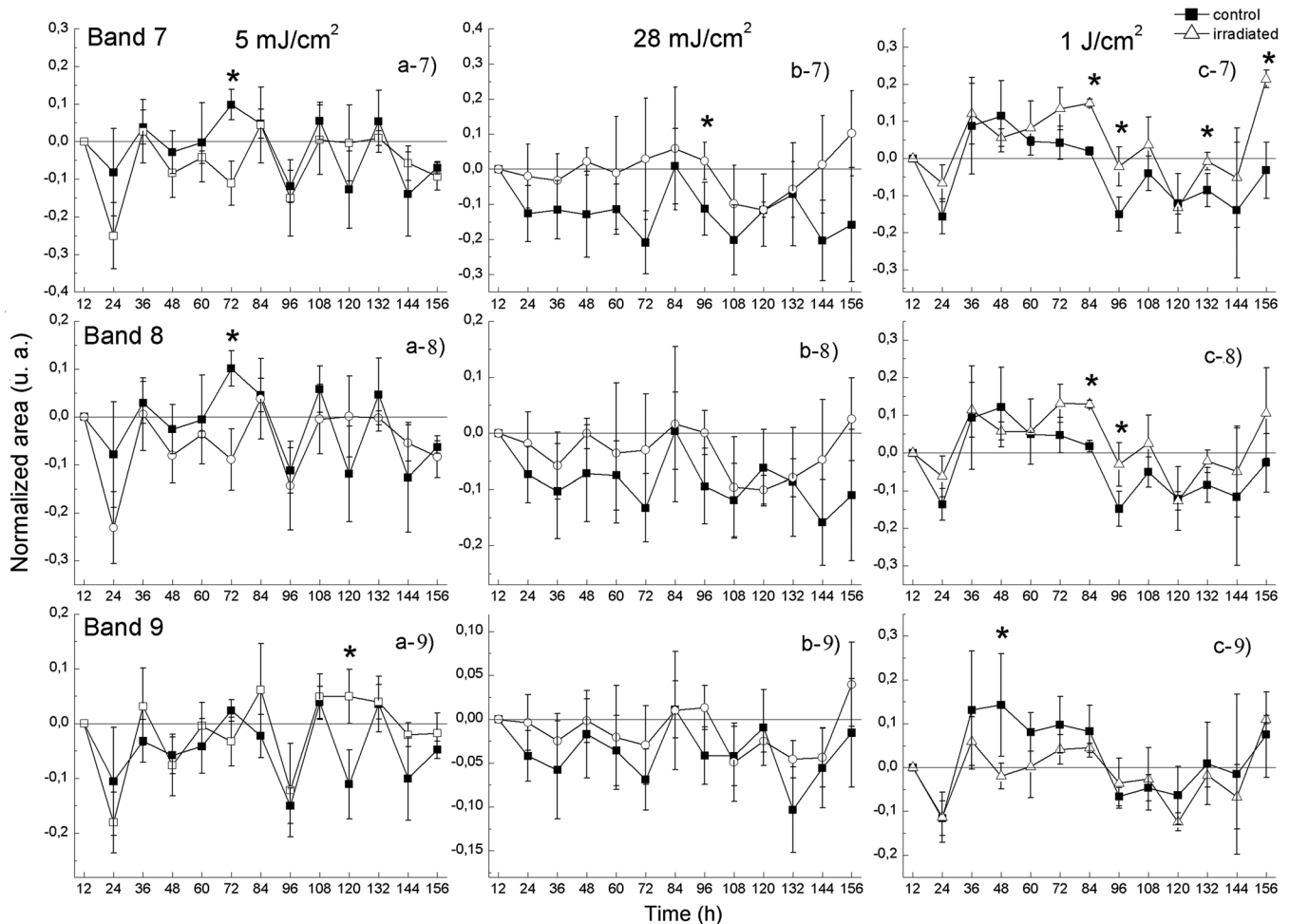


Fig. 7 Normalized areas of bands 7, 8, and 9 with time, where the filled symbols are the control groups and the open symbols are the irradiated groups. Asterisks represent significant differences between the control and irradiated groups.

bands are related to serine, threonine, and tyrosine residues and to phosphorylation.²⁹ There was a decrease in the methyl groups [Fig. 7(a-7), 7(a-8)] compared with the control, whereas the band of amide II [Fig. 7(a-9)] were only slightly lower than those of the control. The decrease of the intensities of the DNA and protein bands with respect to the control group indicates that they were metabolically active but had a decrease due to the light stimulus.³⁰ The decrease in the intensities of the serine and threonine residues and the phosphodiester bands are probably related to the oxidation of nutrients and the formation of ATP,³¹ and the decrease of methylation is related to the regulation of the gene expression.³² All of these events are the result of the decrease of the viability of the cells. On the basis of the mechanisms proposed in the literature⁴ (Fig. 1), we suggest some pathways to explain the results of our experiments. For the fluence of 5 mJ/cm², the pathway is indicated by the number 1, and our assumption is that, due to inhibition, the pathway was related to the production of ROS in mitochondria, which inhibited mitochondrial respiration, leading directly (without transcription factors) to the decrease in metabolism and gene expression. Figure 3 shows that there were not very great differences in the Trypan Blue excluding test for this fluence between the control and irradiated cells, but FTIR spectroscopy is a sensitive tool for comparing two groups of cells, and it

revealed significant differences between some biochemical components of the 5 mJ/cm² irradiated and control cells. The experiments were performed using a spatial filter; thus we ensured that all cells received the same intensity because of the homogenization of the wavefront. The spatial filter has been demonstrated to be so efficient that it had a significant influence on the response of irradiated fibroblasts with different setups, as shown in Ref. 33. Thus, even with few differences, the results of the Trypan Blue excluding test support our assumption that there is bioinhibition at this fluence.

3.2 Discussion for the Mechanism Occurring at a Fluence of 28.8 mJ/cm²

To the best of our knowledge, there are no results at this fluence reported in the literature. For this fluence, the cell viability results showed no proliferative effects. Despite the lack of proliferation, the areas of the bands of DNA [band 1, Fig. 5(b-1)], RNA [band 2, Fig. 5(b-2)], and serine, threonine and tyrosine residues [Fig. 5(b-3)] that could be phosphorylated increased with respect to the control group. Due to the lack of proliferation, one could infer that this increase is stimulated by light. We note that the pathway is illustrated by the arrows marked with the number 2 in Fig. 1. Our assumption is that the phosphate

band increased as a result of the phosphorylation of serine and threonine residues and the increase of ATP, which triggers the production of enzymes and metabolites as well as some methylation, indicating an increase in gene expression because the reduced gene silencing and increased RNA are the result of an increase in the general metabolism. Thus a proposed mechanism at this fluence is one that has no interaction with transcription factors in the nucleus, such as NF- κ B and AP-1, and thus has no influence on proliferation.

3.3 Discussion for the Mechanism Occurring at a Fluence of 1 J/cm²

A clearly proliferative effect due to light stimuli was verified by the increase of band areas with respect to the control group, especially those related to the nucleic acids [band 1, Fig. 5(c-1)] and RNA [Fig. 5(c-2)]. There was also an increase in the phosphorylation of serine, threonine, and tyrosine residues²⁹ [Fig. 5(c-3), 6(c-1)] as well as methylation by gene regulation³² [Fig. 7(c-7), 7(c-8)]. A slight increase in amide II [Fig. 7(c-9)] was observed. This result indicates there was an increase in the metabolic activity and proliferation in this case. An effect of proliferation was found in A2058 human melanoma cells irradiated with a He-Ne laser at 632.8 nm (output power 10 mW): relative to the nonirradiated group, there was a measured increase in intracellular ATP, cytochrome c oxidase, the membrane potential, cAMP, and protein kinase phosphorylation immediately after irradiation (Ref. 34). Our results for cell viability are probably similar to those in the literature because similar cell types were used (cancer) and those also presented cell proliferation. The assumed pathway is indicated by the arrows marked with the number 3 in Fig. 1. A proposed pathway for this fluence includes signaling pathways via agents of nuclear signaling, NF- κ B and AP-1 because of the observed proliferation and the moderate increase in metabolism.

4 Conclusions

Light influenced cell metabolism and viability, depending on the fluence, for a period of at least 6.5 days. For the 5 mJ/cm² fluence, bioinhibition and a decrease of the cell metabolism were observed; for 28.8 mJ/cm², there was no proliferation, but there was an increase of the cell metabolism; and for the 1 J/cm² fluence, cell biostimulation with an increase of cellular metabolism was observed. We have observed three different results for three different fluences, and we suggest that there are three specific mechanisms of interaction between light and cells that are activated at each fluence. Thus these mechanisms are dependent on the fluence. The proposed mechanisms are the production of ROS in mitochondria for 5 mJ/cm², which inhibited mitochondrial respiration; a mechanism that probably has no interaction with transcription factors in the nucleus such as NF- κ B and AP-1 for 28.8 mJ/cm²; and finally, for 1 J/cm², we propose a mechanism that includes signaling pathways via the agents of nuclear signaling, NF- κ B and AP-1.

Acknowledgments

We would like to acknowledge the sponsorships of the CAPES, CNPq, and FAPESP agencies. We are also grateful to the Multiuser Central Facilities from UFABC.

References

1. M. Hamblin and T. Deminova, "Mechanisms of low level light therapy," *Proc. SPIE* **6140**, 614001 (2006).
2. A. Renno et al., "The effects of laser irradiation on osteoblast and osteosarcoma cell proliferation and differentiation in vitro," *Photomed. Laser Surg.* **25**(4), 275–280 (2007).
3. Y.-Y. Huang et al., "Comparison of cellular responses induced by low level light in different cell types," *Proc. SPIE* **7552**, 75520A (2010).
4. T. Karu, "Mitochondrial signaling in mammalian cells activated by red and near-IR radiation," *Photochem. Photobiol.* **84**(5), 1091–1099 (2008).
5. T. Karu, "Mitochondrial mechanisms of photobiomodulation in context of new data about multiple roles of ATP," *Photomed. Laser Surg.* **28**(2), 159–160 (2010).
6. N. Avadhani and R. Butow, "Mitochondrial signaling: the retrograde response," *Mol. Cell* **14**(1), 1–15 (2004).
7. T. I. Karu, L. V. Pyatibrat, and G. S. Kalendo, "Photobiological modulation of cell attachment via cytochrome c oxidase," *Photochem. Photobiol. Sci.* **3**(2), 211–216 (2004).
8. T. I. Karu et al., "Absorption measurements of a cell monolayer relevant to phototherapy: reduction of cytochrome c oxidase under near IR radiation," *J. Photochem. Photobiol. B: Biol.* **81**(2), 98–106 (2005).
9. T. I. Karu, L. V. Pyatibrat, and N. I. Afanasyeva, "A novel mitochondrial signaling pathway activated by visible-to-near infrared radiation," *Photochem. Photobiol.* **80**(2), 366–372 (2004).
10. S. Wu et al., "High fluence low-power laser irradiation induces mitochondrial permeability transition mediated by reactive oxygen species," *J. Cell. Physiol.* **218**(3), 603–611 (2009).
11. J. Tafur and P. Mills, "Low intensity light therapy: exploring the role of redox mechanisms," *Photomed. Laser Surg.* **26**(4), 323–328 (2008).
12. R. Lubart et al., "A low-energy laser irradiation promotes cellular redox activity," *Photomed. Laser Surg.* **23**(1), 3–9 (2005).
13. F. Schwartz et al., "Effect of helium neon laser irradiation on nerve growth factor synthesis and secretion in skeletal muscle cultures," *J. Photochem. Photobiol. B Biol.* **66**(3), 195–200 (2002).
14. T. Karu, "Derepression of the genome after irradiation of human lymphocytes with He-Ne laser," *Laser Therapy* **4**(1), 5–24 (1992).
15. S. Passarella et al., "Increase of proton electro-chemical potential and ATP synthesis in rat liver mitochondria irradiated in vitro by helium-neon laser," *FEBS Lett.* **175**(1), 95–99 (1984).
16. T. Karu et al., "Effect of irradiation with monochromatic visible light on camp content in Chinese hamster fibroblasts," *Il Nuovo Cimento D* **9**(10), 1245–1251 (1987).
17. J. Griffin and J. Shockcor, "Metabolic profiles of cancer cells," *Nature Rev. Cancer* **4**(7), 551–561 (2004).
18. M. Diem et al., "Infrared spectroscopy of cells and tissues: shining lights onto a novel subject," *Appl. Spectrosc.* **53**(4), 148–161 (1999).
19. H. Holman et al., "IR spectroscopic characteristics of cell cycle and cell death probed by synchrotron radiation based Fourier transform IR spectromicroscopy," *Biopolymers* **57**(6), 329–335 (2000).
20. W. Yang et al., "In situ evaluation of breast cancer cell growth with 3D ATR-FTIR spectroscopy," *Vib. Spec.* **49**(1), 64–67 (2009).
21. M. N. Meissel et al., "Effect of the He-Ne laser radiation on the reproduction rate and protein synthesis of the yeast," *Laser Chem.* **5**(1), 27–33 (1984).
22. C. Lucas et al., "Wound healing in cell studies and animal model experiments by low laser therapy: were clinical studies justified? A systematic review," *Lasers Med. Sci.* **17**(2), 110–134 (2002).
23. B. Alberts et al., Chaps. 17 and 24 in *Molecular Biology of The Cell*, 3rd ed., Garland Science, New York (1994).
24. ATCC: American Type Culture Collection, HTB-22 product description, 2012, <http://www.atcc.org/ATCCAdvancedCatalogSearch/ProductDetails/tabid/452/Default.aspx?ATCCNum=HTB-22&Template=cellBiology>.
25. Z. Movasaghi, S. Rehman, and I. Rehman, "Fourier transform infrared (FTIR) spectroscopy of biological tissues," *Appl. Spec. Rev.* **43**(2), 134–179 (2008).
26. N. Lukyanova et al., "Molecular profile and cell cycle in MCF-7 cells resistant to cisplatin and doxorubicin," *Exp. Oncol.* **31**(2), 87–91 (2009).
27. R. Sutherland, R. Hall, and I. Taylor, "Cell proliferation kinetics of MCF-7 human mammary carcinoma cells in culture and effects of

- tamoxifen on exponentially growing and plateau-phase cells," *Cancer Res.* **43**(9), 3998–4006 (1983).
28. M. Diem et al., "A decade of vibrational micro-spectroscopy of human cells and tissue (1994–2004)," *Analyst* **129**(10), 880–885 (2004).
29. M. Meurens et al., "Breast cancer detection by Fourier transform infrared spectrometry," *Vibrat. Spect.* **10**(2), 341–346 (1996).
30. J. T. Eells et al., "Mitochondrial signal transduction in accelerated wound and retinal healing by near-infrared light therapy," *Mitochondrion* **4**(5–6), 559–567 (2004).
31. K. Lin et al., "An ATP-site on-off switch that restricts phosphatase accessibility of AKT," *Sci. Signall.* **5**(223), ra37 (2012).
32. W. Doerfler et al., "DNA methylation—a regulatory signal in eukaryotic gene expression," *J. Gen. Virol.* **57**(1), 1–20 (1981).
33. T. D. Magrini, A. R. Santos, Jr., and H. S. Martinho, "Standardization of experimental parameters for LLLT studies," *Proc. SPIE* **8211**, 821106 (2012).
34. W. P. Hu et al., "Helium-neon laser irradiation stimulates cell proliferation through photostimulatory effects in mitochondria," *J. Invest. Dermatol.* **127**(8), 2048–2057 (2007).